Immunity, Vol. 21, 817–830, December, 2004, Copyright ©2004 by Cell Press

Generalized Resistance to Thymic Deletion in the NOD Mouse: A Polygenic Trait Characterized by Defective Induction of *Bim*

Adrian Liston,[1] Sylvie Lesage,[1,9] Daniel H.D. Gray,[2] Lorraine A. O'Reilly,[3] Andreas Strasser,[3] Aude M. Fahrer,[4] Richard L. Boyd,[2] Judith Wilson,[1] Alan G. Baxter,[5] Elena M. Gallo,[6] Gerald R. Crabtree,[6] Kaiman Peng,[7] Susan R. Wilson,[8] and Christopher C. Goodnow[1,*]

[1]Immunogenomics Laboratory
John Curtin School of Medical Research and
The Australian Phenomics Facility
The Australian National University
Canberra, 2601
Australia

[2]Department of Pathology and Immunology
Faculty of Medicine
Monash University
Melbourne, 3181
Australia

[3]The Walter and Eliza Hall Institute of Medical Research
Melbourne, 3050
Australia

[4]Biochemistry and Molecular Biology
The Australian National University
Canberra, 2601
Australia

[5]Comparative Genomics Centre
James Cook University
Townsville, Queensland 4811
Australia

[6]Department of Microbiology and Immunology
Beckman Center, Room B211
Stanford, California 94305

[7]Biomolecular Resource Facility
John Curtin School of Medical Research
The Australian National University
Canberra, 2601
Australia

[8]Mathematical Sciences Institute
John Dedman Mathematical Sciences
The Australian National University
Canberra, 2601
Australia

Summary

The cause of common polygenic autoimmune diseases is not understood because of genetic and cellular complexity. Here, we pinpoint the action of a subset of autoimmune susceptibility loci in the NOD mouse strain linked to *D1mit181*, *D2mit490*, *D7mit101*, and *D15mit229*, which cause a generalized resistance to thymic deletion in vivo that applies equally to *Aire*-induced organ-specific gene products in the thymic medulla and to systemic antigens expressed at high levels throughout the thymus and affects $CD4^+$, $CD4^+8^+$, and $CD4^+25^+$ thymocytes. Resistance to thymic deletion does not reflect a general deficit in TCR signaling to calcineurin- or ERK-induced genes, imbalance in constitutive regulators of apoptosis, nor excessive signaling to prosurvival genes but is distinguished by failure to induce the proapoptotic gene and protein, Bim, during in vivo encounter with high-avidity autoantigen. These findings establish defects in thymic deletion and Bim induction as a key mechanism in the pathogenesis of autoimmunity.

*Correspondence: chris.goodnow@anu.edu.au
[9]Present address: Immunoregulation, CHUM Research Centre, Montreal University, Montreal, H2L 4M1, Canada.

Introduction

Autoimmune diseases directed against different target tissues often cluster together in individuals and families and in the inbred nonobese diabetic (NOD) mouse strain and its relatives, leading to the view that they arise from a shared, general susceptibility toward autoimmunity with the specific target antigens and tissues varying depending upon additional genetic traits such as the MHC and upon specific environmental factors (Todd and Wicker, 2001). The basis for such a generalized autoimmune propensity is not known but could have two not mutually exclusive origins. First, there may be an intrinsic reduction in the active processes for eliminating or silencing clones of T or B lymphocytes that bear receptors with dangerously high affinity for self antigens. Second, intrinsic hyperreactivity of target tissues or immune cells could exaggerate responses by lower affinity self-reactive lymphocytes that normally fall below the threshold for actively acquired tolerance and might otherwise exist in a state of immunological ignorance.

Defects in actively acquired tolerance by thymic clonal deletion apparently explain the cluster of autoimmune diseases in the rare Mendelian disorder, Autoimmune Polyendocrine Syndrome 1, in humans or mice with homozygous loss of function mutations in the Autoimmune Regulator (*Aire*) gene. *Aire* is not required within autoreactive T cells themselves but is required for ectopic expression of organ-specific gene products such as insulin within the radioresistant thymic epithelial stroma (Anderson et al., 2002), and in the absence of *Aire*, organ-specific T cells fail to be deleted in the thymus (Liston et al., 2003). Defects in thymic clonal deletion have also been associated with the non-MHC-linked genetic susceptibility to autoimmune diabetes in the NOD mouse (Kishimoto and Sprent, 2001; Lesage et al., 2002). Kishimoto and Sprent showed that semimature thymocytes from NOD, intermediate between the immature $CD4^+8^+$ DP cells and $CD4^+8^-$ SP cells, are relatively resistant to cell death in vitro when their TCRs are cross-linked with different doses of anti-TCR antibody, although this finding has been disputed (Villunger et al., 2003). Lesage et al. analyzed thymic deletion in vivo, tracing differentiation of T cells bearing a high affinity TCR for peptide 46–61 of hen egg lysozyme (HEL) bound to $I\text{-}A^k$ in TCR and insulin promoter:HEL double transgenic mice backcrossed to $H2^k$ congenic NOD or B10

strains (Lesage et al., 2002). These cells were deleted during the transition between DP and SP cells in the thymus of autoimmune resistant B10.Br strain mice, but not in the NOD.*H2*^{k} strain where the T cells escaped to the periphery and progression to diabetes ensued. The NOD defect in thymic deletion was comparable in magnitude to that caused by deficiency of *Aire* in the same model (Liston et al., 2003); however, the NOD defect acted cell autonomously within autoreactive T cells carrying the non-MHC NOD genes (Lesage et al., 2002). This in vivo NOD defect in negative selection has recently been extended to the CD8$^+$ thymocyte population in the AI4 transgenic model, indicating that it is not isolated to the CD4$^+$ lineage alone nor to the 3A9 transgene (Choisy-Rossi et al., 2004).

The basis for T cell resistance to thymic deletion in NOD mice is unknown. It is not known if this resistance is uniquely associated with thymic deletion to *Aire*-induced antigens encountered late in differentiation in the thymic medulla or if it might relate to the systemic autoimmune syndromes that also occur in NOD strains nor is it known if this defect explains the action of one or more of the twenty-two known insulin dependent diabetes (*Idd*) or other autoimmune susceptibility loci in NOD. Here, we analyze these issues by a combination of in vivo cellular, molecular, and genetic approaches and find that there is a global, quantitative decrease in the efficiency of clonal deletion within the DP, SP, and CD4$^+$25$^+$ thymocyte subsets across a range of amounts, locations, and sources of antigen. In molecular terms, the defect is explained by selectively diminished induction of *Bim* and reflects the additive action of four NOD loci, previously largely associated with diabetes and other autoimmune disorders in NOD mice and encompassing the *Bim* locus itself.

Results

Defective Thymic Deletion to Four Different Sources of Autoantigen

Thymic deletion of T cells bearing NOD or B10 genetic makeup was analyzed in vivo across a range of sources and amounts of thymic antigen to determine if NOD resistance to thymic deletion was limited to particular stages of development and sources of antigen. Four different HEL transgenic strains were backcrossed to 3A9 TCR transgenic mice on the B10.Br and NOD.*H2*^{k} (NODk) MHC-congenic strain backgrounds. The ins:mHEL transgenic strain synthesizes high concentrations of membrane bound HEL as a self antigen in pancreatic islet β cells under control of the rat insulin promoter (Akkaraju et al., 1997b). Trace quantities of cleaved soluble HEL (sHEL) are present in the circulation of these mice (Akkaraju et al., 1997b), and *Aire*-dependent ectopic expression occurs in the thymus (Liston et al., 2004) with trace immunofluorescent staining in rare medullary cells (Figure 1). The Tg-HEL transgenic strain encodes the same membrane bound HEL protein under the control of a fragment of the rat thyroglobulin promoter, resulting in high expression in the thyroid epithelium, undetectable levels of sHEL present in the circulation (Akkaraju et al., 1997a, 1997b), and expression in scattered thymic medullary epithelium detected by immunofluorescence (Figure 1) associated with *Aire*-dependent deletion (Liston et al., 2004). The Mt:sHEL transgenic strain ML4 encodes soluble HEL driven by the metallothionein promoter giving only a trace basal expression in the serum (Adelstein et al., 1991) and immunofluorescent staining in medullary epithelial cells comparable to the thyroglobulin promoter (Figure 1), although this is predominantly *Aire*-independent (A.L., unpublished data). The H2-K:mHEL transgenic strain encodes the membrane bound form of HEL being expressed under the H2-K^b promoter, driving ubiquitous high-level expression on radioresistant cells and thymocytes (Figure 1; Hartley et al., 1991), and is unaffected by *Aire* mutations (Liston et al., 2004). For each transgene, HEL expression in the thymus was equivalent on the B10.Br and NODk backgrounds as measured by immunofluorescence (Figure 1; histograms shown in Supplemental Figure S1 available online at http://www.immunity.com/cgi/content/

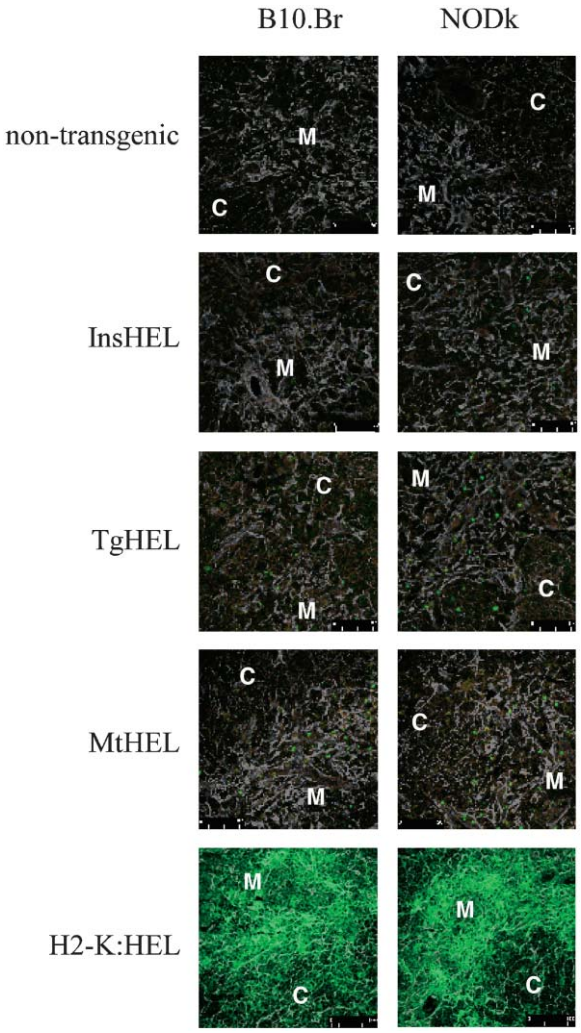

Figure 1. HEL Protein Expression in Thymi of Transgenic Mice

Sections of frozen thymi from nontransgenic, insHEL, TgHEL, MtHEL, and H2-K:HEL transgenic B10.Br and NODk mice were stained with antibodies to HEL (green) and keratin (gray) and examined by confocal microscopy. The thymic medulla (M) and cortex (C) are indicated. Data are representative of three experiments.

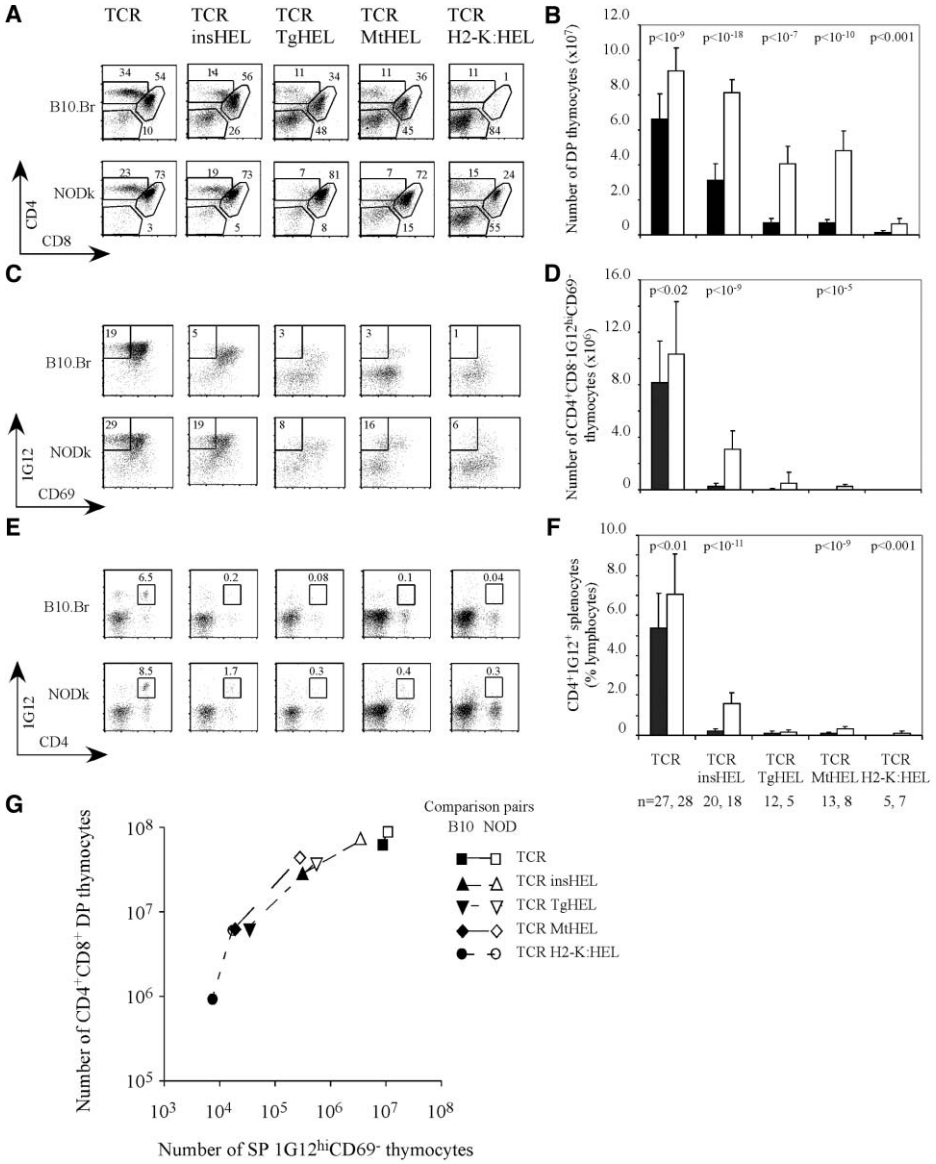

Figure 2. Cellular Effects of Thymic HEL Expression on 3A9 T Cells in B10.Br and NODk Genetic Backgrounds

Development of 3A9 TCR-bearing cells was analyzed by flow cytometry in TCR transgenic and the indicated TCR×HEL double transgenic mice on the B10.Br and NODk backgrounds. (A) Representative CD4 versus CD8 profiles of thymocytes. (B) Mean number of $CD4^+CD8^+$ double positive thymocytes. B10.Br strains are shown in black, NODk strains are shown in white, error bars represent the SD. Significance of differences between B10.Br and NODk groups of the same genotype are indicated by t test p values about the group. (C) Representative profiles showing staining with the 3A9 TCR clonotypic-specific antibody 1G12 and CD69, gated on $CD4^+CD8^-$ SP thymocytes. (D) Mean number of mature $CD69^-$ $1G12^{hi}$ $CD4^+$ single positive thymocytes. Significance of differences between B10.Br and NODk groups of the same genotype are indicated by t test p values above the group. (E) CD4 and clonotypic 1G12 staining within splenic lymphocytes. (F) Mean percentage of splenocytes that are $CD4^+1G12^+$. Significance of differences between B10.Br and NODk groups of the same genotype are indicated by t test p values above the group. (G) A pairwise comparison of NODk and B10.Br counterparts, illustrating the relative deletion of immature ($CD4^+CD8^+$) and mature ($CD4^+CD8^-1G12^+CD69^-$) cells under each condition and showing the resistance to deletion in each of the NODk transgenic strains (open symbols) relative to their B10.Br counterparts (closed symbols) for the same concentration of thymic HEL.

full/21/6/817/DC1/) as were serum levels of sHEL protein (data not shown).

While there was no detectable effect of the NOD strain background upon thymic antigen expression, we next investigated how the NOD versus B10 background affected thymic deletion in TCR×HEL double transgenic mice bearing each of the HEL transgenes (Figure 2). T cell differentiation was traced by four color flow cytometry, measuring CD4 and CD8 expression to distinguish the major subsets (Figure 2A), with further subdivision of the $CD4^+$ SP subset based on staining with the 1G12 antibody specific for the 3A9 $\alpha\beta$ TCR clonotype and for CD69 (Figure 2C). Large numbers of mature $1G12^{hi}CD69^-$ SP cells and semimature $CD4^+$ $1G12^{hi}CD69^+$ SP cells were present in the thymus of B10.Br and NODk 3A9 transgenic mice in the absence of HEL (Figure 2D). In TCR×HEL double transgenic mice carrying the different HEL transgenes, these SP subsets and the DP cells

underwent graded degrees of clonal deletion as gauged by decreased cell frequency and absolute numbers, and in each case, deletion was markedly less efficient in the NOD animals. First, when comparing the numbers of DP cells in double transgenic mice to those in TCR-only controls (Figures 2B and 2G), we found that their number was decreased 50% in B10.Br TCR×insHEL double transgenic mice, whereas no significant decrease was triggered by insHEL in the NOD counterparts. DP cell numbers were reduced more markedly, to 10% of controls, in B10 mice with the thyroglobulin- or metallothionein-regulated transgenes, which are expressed at higher levels in thymic medulla. Deletion of DP cells was now detected in the NOD counterparts but only to the levels achieved in B10 mice with the lower amounts of thymic HEL from the insulin promoter so that five times more DP cells remained. DP cells were almost completely absent in B10 mice with the highly expressed H2-K:HEL transgene (Figure 2A), whereas five times more DP cells again remained in the NOD counterparts so that deletion only attained the levels observed in B10 mice with the much less expressed TgHEL or MtHEL transgenes (Figures 2B and 2G).

In the same panel of mice, thymic deletion of mature $CD4^+CD8^-1G12^{hi}CD69^-$ cells (Figure 2C) was also graded but appeared more efficient than in the DP subset and exhibited an even greater magnitude of defect in the NOD counterparts (Figures 2D and 2G). Mature HEL-reactive thymocytes were reduced to 3% of control numbers in insHEL mice on the B10.Br background, whereas they were only decreased to 30% of controls in the NODk background so that more than ten times as many autoreactive cells remained. In the Tg and Mt transgenic strains with higher HEL expression in the thymic medulla, mature cells were decreased to ~0.3% of controls, whereas fifteen times higher numbers remained in the NOD counterparts so that deletion only attained the efficiency of B10 animals with insHEL. In the H2-K:HEL animals, the numbers of mature cells in the NOD group were reduced to 0.2% of controls, but this magnitude compared only with the B10 animals expressing much less thymic HEL from Tg or Mt transgenes. The generalized decrease in efficiency of clonal deletion was also apparent when peripheral $CD4^+1G12^+$ cells were enumerated in the spleen (Figures 2E and 2F). When the mean number of DP and mature SP cells in the thymus were plotted, the relationship between deletion in DP and mature cell subsets appears unchanged by the NOD background, but deletion is shifted up the curve by between 5- and 15-fold for each source of antigen (Figure 2G). Thus, the NOD thymic deletion defect is not limited to organ-specific promoters expressed in thymic medulla but manifests at early and late stages of maturation and low or high amounts of thymic autoantigen.

Defective Thymic Enrichment of $CD4^+25^+$ Cells

As an alternative to clonal deletion, thymic encounter with autoantigen can also result in apparent conversion of autoreactive CD4 cells to $CD25^+$ regulatory cells that are exported from the thymus rather than being deleted (Jordan et al., 2001). Consistent with these results is the finding that a much greater fraction of $CD4^+1G12^+$ SP thymocytes are $CD25^+$ when a HEL transgene is present (Figure 3A), and this proportion plateaus at >50% of the autoreactive SP cells in Tg, Mt, and H2-K mice on the B10 background with the higher levels of thymic HEL (Figure 3B). In the NOD counterparts of these animals; however, little increase in the proportion of $CD25^+$ cells occurred under the insulin promoter, rising to 30% in the Tg and Mt animals and only reaching the plateau of 50% in the H2-K animals. The increase in proportion of $CD4^+$ cells that bear the CD25 marker is nevertheless not due to any increase in absolute number of this subset, because the thymic presence of HEL actually results in a decrease in the absolute number of mature $CD25^+$ thymocytes (Figure 3C). The same increase in proportion, but not absolute numbers, of $CD25^+$ cells with the presence of self-antigen is also observed in TCR×insHEL double transgenic B10.Br $TCR\alpha^{0/0}$ and $RAG^{0/0}$ mice, establishing that these cells do not require another receptor chain for their formation (data not shown). Plotting the relationship between mean numbers of $CD25^+$ and $CD25^-$ $CD4^+1G12^+$ cells in the different groups reveals that the $CD25^+$ population appears remarkably refractory to thymic deletion and only shows evidence for a numerical reduction in B10 strains with higher thymic antigen expression (Figure 3D).

NOD Effects on Gene Responses Mediating Negative and Positive Selection

The data above indicate a general, quantitative decrease in the efficiency of clonal deletion affecting three key thymocyte subsets. Because the NOD effect acts cell autonomously within the T cells, it could arise from a global reduction in efficiency of TCR signal transmission, heightened signaling to prosurvival pathways, selective decrease in TCR signaling of apoptosis, or a shift in the balance of pro- and antiapoptotic effectors. To resolve these alternatives, we gauged their in vivo activity before and during negative or positive selection by flow sorting discrete subsets of thymocytes from NOD and B10 counterparts and then measuring mRNAs for genes that are well-defined targets and mediators of these processes. Four subsets of thymocytes were sorted from both B10.Br and NODk counterparts (Figure 4A). The subset of DP cells that are negative for CD69 and 1G12 TCR clonotype ("early DP") was sorted from TCR and TCR×insHEL double transgenic mice to obtain cells that had not yet received positive or negative selection signals. Cells that were in the early stages of positive selection ("early SP") were sorted from TCR animals lacking HEL based upon the cell surface phenotype of $CD4^+CD8^{low}CD69^+1G12^+$, and cells in the early stages of negative selection ("early SP") were sorted based on the same phenotype from double transgenic animals. These four types of cells were sorted from multiple NOD or B10 animals under conditions designed to prevent any gene induction ex vivo to yield three biologically and technically independent pools of mRNA for each of the eight experimental groups. After RNA purification and double amplification, labeled cRNA was hybridised to Affymetrix 430A GeneChips, and the data analyzed by MAS software.

The microarray dataset was first verified by analyzing relative mRNA values for genes with a well-established role and expression pattern during thymocyte maturation, either decreasing during differentiation from DP to SP cells (*Cd8*, *Rag1*, *Rag2*, and *preT*α, Figure 4B) or

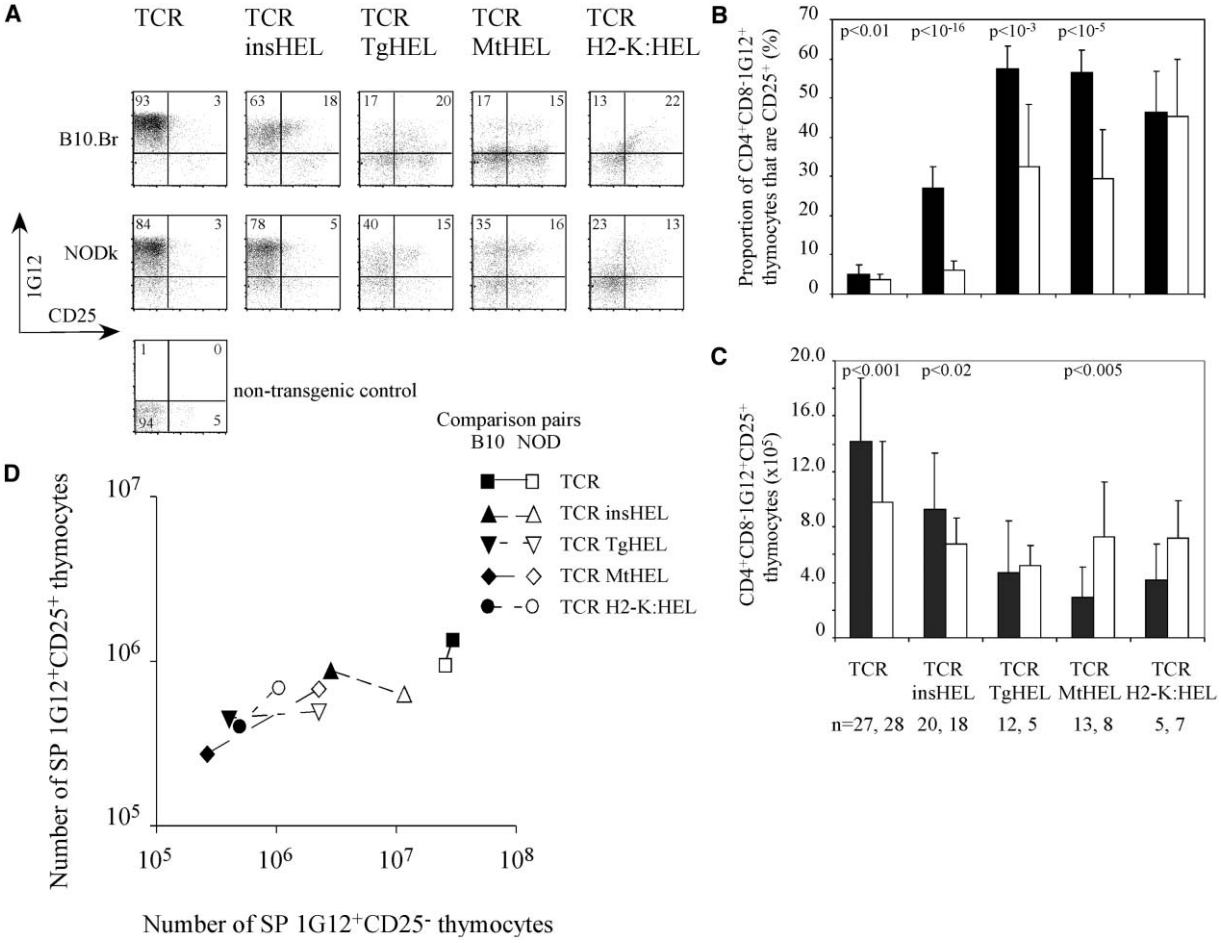

Figure 3. Production of $CD4^+CD25^+$ Thymocytes in B10.Br and NODk Transgenic Strains

TCR and double transgenic mice on the B10.Br and NODk backgrounds were assessed for $CD4^+CD25^+$ thymocyte production by flow cytometry. (A) Representative profiles for CD25 versus 1G12 clonotype, gated on $CD4^+$ SP thymocytes. (B and C) Mean percentage (B) and number (C) of mature $CD4^+CD8^-1G12^+$ thymocytes expressing CD25. B10.Br strains are shown in black, NODk strains are shown in white. Error bars represent the SD. Significance of differences between B10.Br and NODk groups of the same genotype are indicated by t test p values about the group. (D) A pairwise comparison of NODk and B10.Br counterparts, illustrating the relative deletion of $CD25^+$ and $CD25^-$ semimature ($CD4^+CD8^-1G12^+$) thymocytes under each condition and showing the resistance to deletion in each of the NODk transgenic strains (open symbols) relative to their B10.Br counterparts (closed symbols) for the same concentration of thymic HEL.

increasing in SP cells (*Cd4*, *Ccr7*, *S1pr1*, and *Il7Rα*, Figure 4C). Each of these mRNAs showed dramatic and highly reproducible changes in expression between DP and SP cell populations as expected with minor differences between negative and positive selecting thymi and between B10 and NOD counterparts.

Considering the data above showing that an increased proportion of $CD4^+1G12^+$ cells are $CD25^+$ in TCR×insHEL animals on the B10 background, we then examined the data for a set of mRNAs established by others as being increased in peripheral $CD4^+25^+$ T regs (McHugh et al., 2001). Consistent with the flow cytometry, *Cd25* mRNA was selectively increased in negatively selecting SP cells from B10 mice, but not in NOD counterparts (Figure 5A). Parallel increases in *Gitrd*, *Pcd1*, *4-1bb*, *Ox40*, and *Ctla4* occurred in negatively selecting SP cells from B10 animals, and these also failed to be increased markedly in the NOD counterparts with the exception of *Ctla4,* which was equally increased in the NOD cells. *Foxp3* mRNA was consistently present only in the B10 negatively selecting population replicates; however, expression levels were too low to identify any consistent changes in the other samples.

Sets of previously identified reporter genes were analyzed to measure the strength of major signaling pathways to address the hypothesis of a global reduction in efficiency of TCR signal transmission. We first examined a set of genes induced by the TCR-calcineurin-NFAT signaling pathway based upon microarray analysis of calcineurin B-deficient thymocytes: *Egr2*, *Ian1*, *Adam19*, *Itgb7*, *CD52*, and *Bach2* (E.G. and G.C., unpublished data). All of these genes showed induction during developmental progression from DP to SP stages, little or no significant difference between positive and negative selection, and no strain differences between B10.Br and NODk (Figure 5B). Because the ras-MEK-ERK-TCF pathway is also activated and required for TCR-mediated positive selection, we examined a set of genes known to be targets of this pathway. *Egr-1, fos, zfp36l1*, and *Nab2* were all induced in early SP cells undergoing positive selection or negative selection (Figure 5C); however, there was again no significant differences between NOD

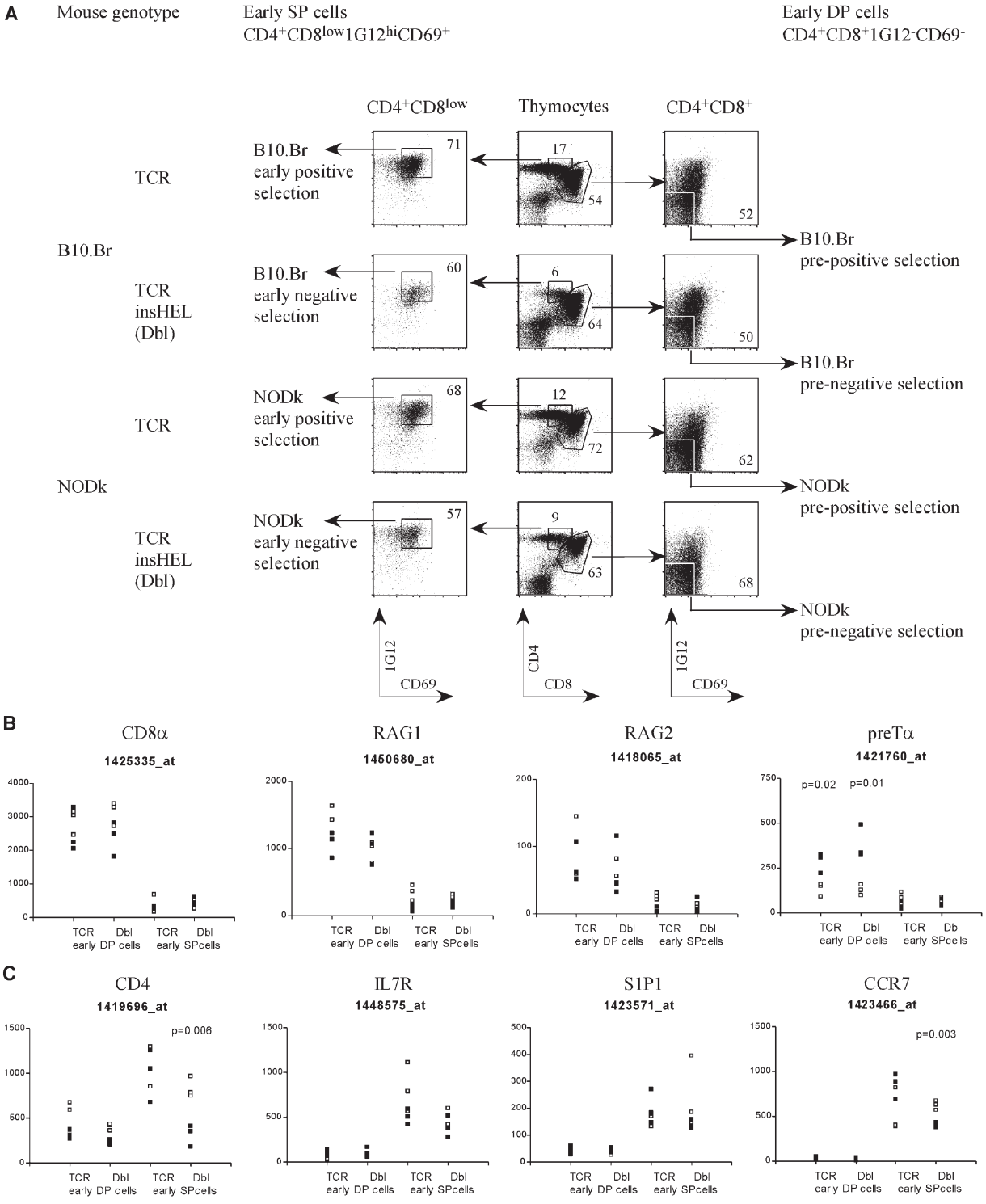

Figure 4. Experimental Design and Verification of Microarray Analysis of Sorted Thymocyte Subsets

(A) Thymocytes from TCR transgenic and TCR:insHEL double transgenic (Dbl) nondiabetic 6- to 8-week-old female mice on the B10.Br and NODk backgrounds were sorted into the indicated subsets. Three biological replicate pools of mRNA were generated for each subset with independent sorts. Because of lower cell numbers, B10.Br Dbl early single positive cells were pooled from multiple independent donor mice. These replicate mRNA pools were independently labeled and hybridized to Affymetrix m430A arrays, and the average expression level for representative genes in each sample is shown by the square symbols in (B) and (C).

(B) Expression levels measured for representative well-characterized genes known to be developmentally downregulated between the early double positive stage and the early single positive stage.

(C) Expression levels of genes that are well established to be developmentally upregulated between the early double positive stage and the early single positive stage. Individual values of biological replicates are represented in black (B10.Br) and white (NODk) boxes.

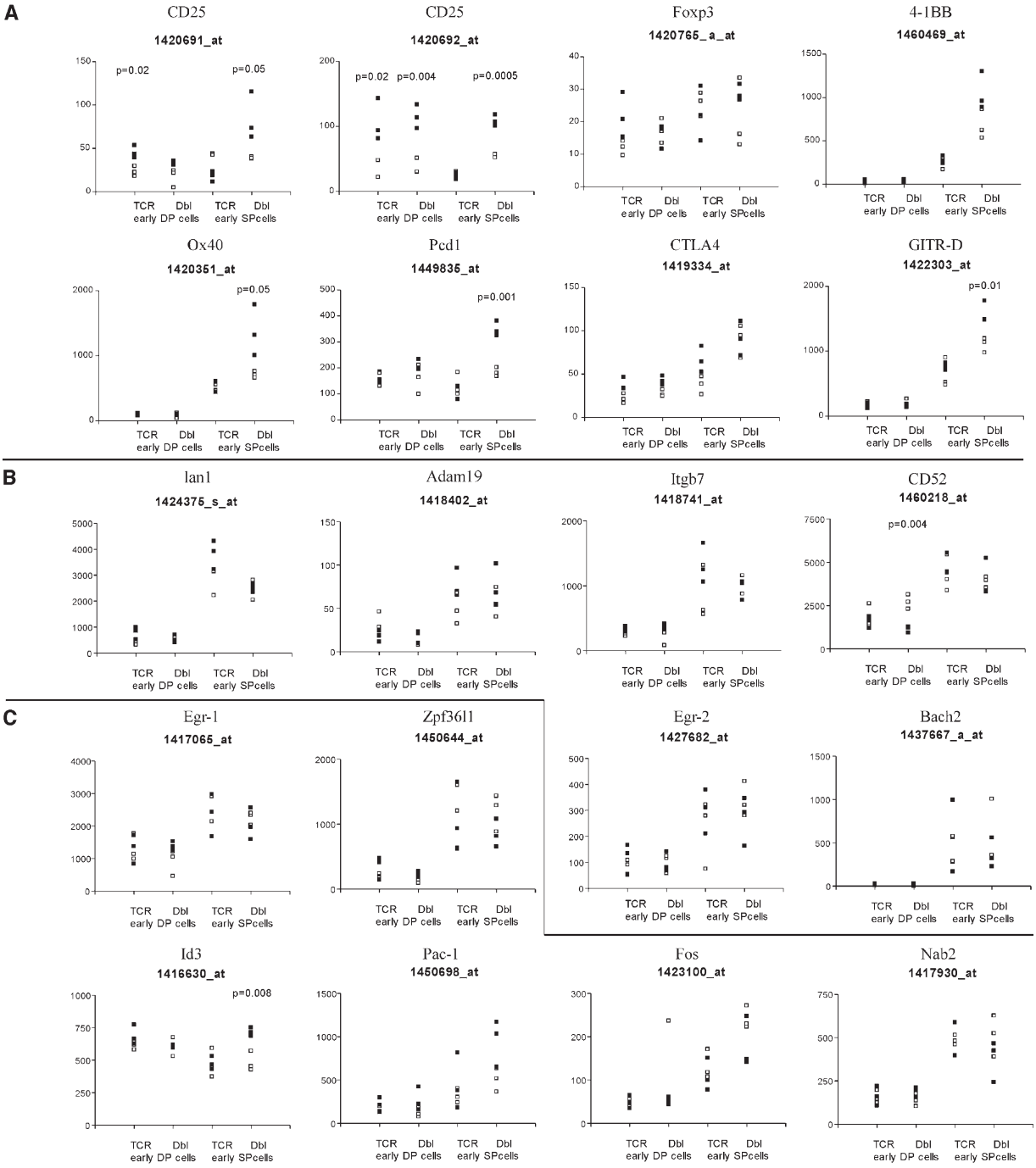

Figure 5. Expression of Known $CD4^+25^+$ Regulatory T Cell Markers and Targets of Calcineurin and Erk Signaling in Thymocytes

(A) Genes known to be increased in $CD4^+CD25^+$ regulatory cell subset.

(B) Calcineurin response genes.

(C) ERK response genes. Individual values are represented in black (B10.Br) and white (NODk) boxes with significant differences between the strain backgrounds indicated above the plot.

and B10 strains. By these downstream measures, both the calcineurin and ERK pathways appear to signal normally during positive and negative selection of NOD thymocytes.

We next tested the alternative hypotheses of selectively heightened signaling to prosurvival pathways, selectively diminished signaling of proapoptotic effectors, or a constitutive shift in the balance of pro- and antiapoptotic terminal regulators. An important prosurvival pathway activated by the TCR comprises various members of the NFκB family. Analysis of *NFκB1/p105, NFκB2, Bcl-3, c-rel, rel-B,* *IκBα*, and *IκBβ* showed that all except *p65/rel A* and *IκBβ* were induced in early SP cells undergoing positive and negative selection,

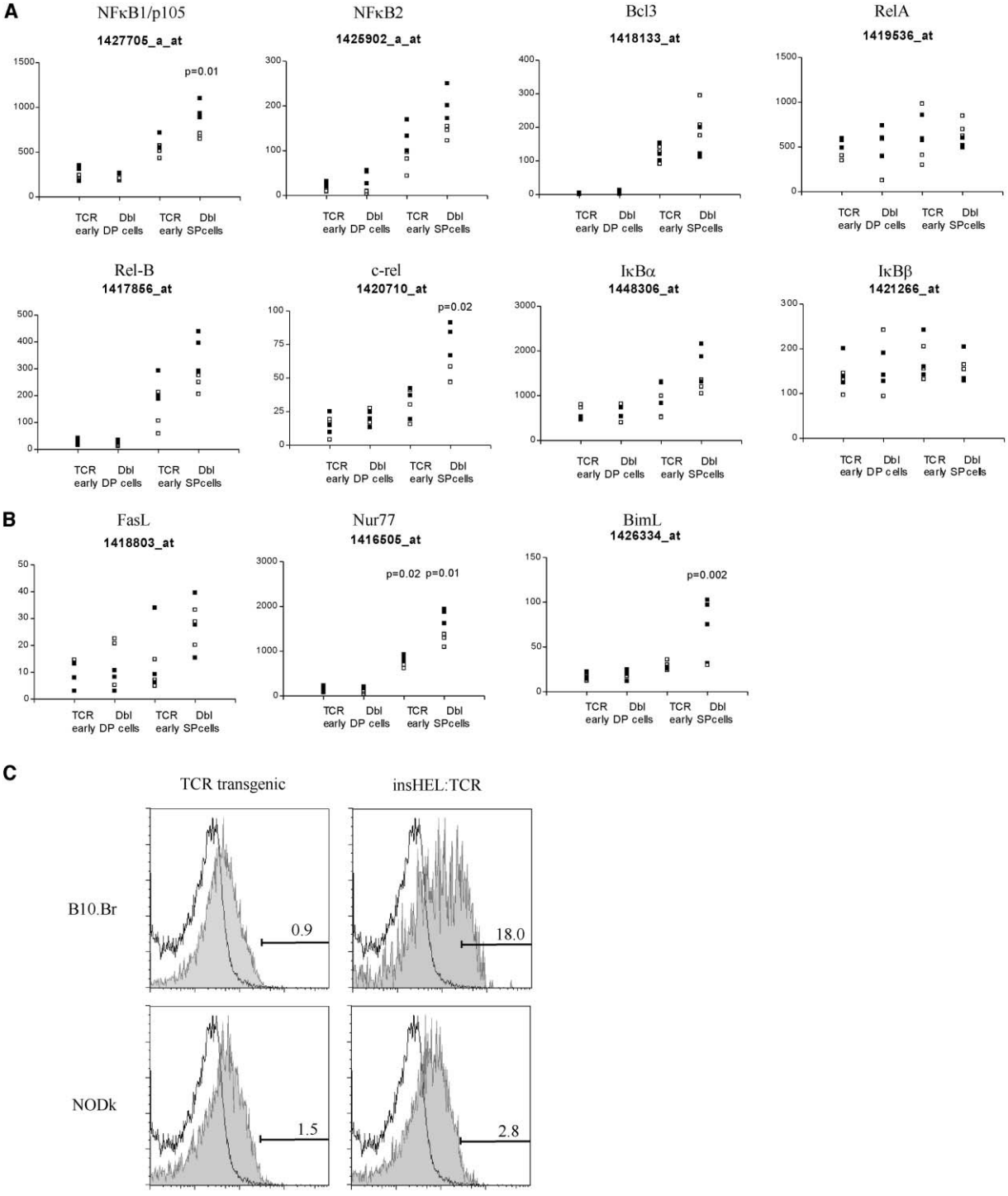

Figure 6. Expression of Genes Known to Regulate Apoptosis

(A) Expression of known antiapoptotic genes.

(B) Known proapoptotic genes. Individual values are represented in black (B10.Br) and white (NODk) boxes with significant differences between the strain backgrounds indicated above the plot.

(C) Flow cytometry analysis of Bim protein (tinted) in $CD4^+1G12^+$ thymocytes, comparing $CD4^+1G12^+$ thymocytes under positive (TCR transgenic) and negative (TCR:insHEL double transgenic) selection on the B10.Br and NODk backgrounds with the percentage of Bim^+ cells indicated on the graph. Staining specificity is indicated through parallel staining of $Bim^{0/0}$ thymocytes (line, background of 0.8% Bim^+ cells).

generally to highest levels in negative selection (Figure 6A). None were significantly overinduced in NODk thymocytes compared with B10 counterparts, and, in fact, *NFκB1/p105* and *c-rel* were less induced in NODk early SP cells undergoing negative selection.

Analysis of constitutively expressed pro- and antiapo-

ptotic regulators showed no significant differences in expression of *Bcl-2*, *mcl-1*, *Bax*, *Bak*, *Bad*, *noxa*, *puma*, *caspase 9*, *caspase 3*, and *apaf-1* in B10.Br and NODk thymocytes (Supplemental Figure S2), arguing against the hypothesis of a shift in favor of constitutive antiapoptotic molecules. Analysis of the components of the TCR-activated Fas apoptotic pathway showed induction of *FasL* in early SP cells undergoing negative selection that was not different between NOD and B10 cells (Figure 6B). Other elements of this pathway—*Fas*, *FADD*, *Casp8*, and *cFlip*—showed no significant induction or strain differences (Supplemental Figure S1). By contrast, analysis of the two TCR-induced genes with clearly established effector roles in thymic deletion, *BimL* and *Nur77*, revealed striking deficits selectively in NOD early SP cells undergoing negative selection. Consistent with previous data (Bouillet et al., 2002; Villunger et al., 2004; Woronicz et al., 1994; Xue et al., 1997), *BimL* and *Nur77* mRNAs were dramatically increased in B10.Br early SP cells undergoing negative selection compared to their positively selecting early SP counterparts (Figure 6B). In negatively selecting early SP cells from NOD, however, there was no measurable increase in *BimL* and a significantly blunted increase in *Nur77*. Because of the essential function of *Bim* as an apoptotic initiator during thymic deletion and previously defined posttranslational regulation (Puthalakath et al., 1999), a flow cytometric assay for intracellular Bim was developed. A monoclonal antibody, 10B12, with high specificity for Bim and no crossreactivity to any other protein (L.A.O., A.S., and D. Huang, unpublished data) was used to measure intracellular Bim levels in fixed and permeabilized $CD4^+1G12^+$ thymocytes. Using the $Bim^{0/0}$ mouse as a staining control (Bouillet et al., 1999), we found Bim at just measurable levels in $CD4^+1G12^+$ thymocytes from the B10.Br and NODk TCR transgenic mice, which was dramatically increased in vivo in SP cells undergoing negative selection from B10.Br TCR:insHEL double transgenic mice (Figure 6C). Double staining for Bim and CD25 showed that increased Bim was limited to the $CD25^-$ subset (data not shown). No detectable increase in Bim protein occurred in the corresponding SP cells in NODk double transgenic mice. Collectively, these results establish that NOD thymocytes have a selective in vivo deficit in autoantigen induction of proapoptotic effectors, in particular Bim.

Genetic Loci Causing Defective Thymic Deletion in NOD

The failure to induce Bim in autoreactive NOD SP thymocytes is sufficient to explain their generalized defect in thymic deletion, because *Bim*-deficient mice have a profound defect in thymocyte negative selection, and loss of a single gene copy causes a marked thymic deletion defect and autoimmunity (Bouillet et al., 1999, 2002; Villunger et al., 2004). We therefore wished to know if resistance to thymic deletion mapped to the *Bim* locus or to a subset of autoimmune loci established previously in the NOD strain. A backcross was established between (B10.Br×NOD.$H2^k$)F1 animals and NOD.$H2^k$ based upon the earlier finding that defective negative selection in NOD is "recessive," because double transgenic F1 mice display efficient negative selection comparable to B10.Br mice (Lesage et al., 2002). In the backcross, the TCR and insHEL transgenes segregated independently in hemizygous state, because neither of these can be fixed as homozygotes. A total of 1906 backcross mice were bred, 979 female offspring weaned and genotyped for HEL and TCR transgenes, and 149 double transgenic backcross animals were identified and their thymus analyzed for efficiency of clonal deletion. As shown in Figures 2 and 3, defective negative selection in the NOD animals is characterized by an increased frequency of $1G12^{hi}CD69^-CD4$ SP cells and by failure to increase the proportion of $CD4^+1G12^+$ cells that are $CD25^+$, so this combination of parameters was used (Figure 7) to classify the 149 TCR×insHEL backcross mice into "deletors" comparable to F1 controls (24%, n = 35), "nondeletors" comparable to NOD controls (35%, n = 52), and intermediates (42%).

Next, the deletor and nondeletor animals were individually genotyped with SSLPs linked to seven major NOD *Idd* loci: *Idd2*, *Idd3/10/18*, *Idd4*, *Idd5*, *Idd6*, *Idd9/11*, and *Idd13/Bim* (Figure 7). Loci with a preponderance of heterozygotes (B10/NOD) in the deletor cluster and homozygotes (NOD/NOD) in the nondeletor cluster, as measured by contingency tables for χ^2 values, were suggestive for linkage to the NOD defect in thymic deletion. Only two of these *Idd* regions showed evidence for linkage: a χ^2 value of 4.6 ($p = 0.03$, not Bayes corrected for multiple testing) at the *Idd5* locus on chromosome 1 (Ch1) at *D1mit181* (42.6 cM) and a χ^2 value of 5.4 ($p = 0.02$, not Bayes corrected) at the *Idd13* locus on Ch2 at *D2mit490* (64.5 cM) which is also linked to the *Bim* gene (59 cM).

A scan of other chromosomal regions was then performed to assess the overall genetic complexity of the trait. This identified two additional NOD-derived regions with highly significant association with resistance to thymic deletion: a χ^2 value of 11.3 centered on Ch7 at *D7mit101* (60 cM on the MGI map) and a χ^2 value of 9.7 centered on Ch15 at *D15mit229* (22 cM). Paradoxically, two loci showed an association between this trait and inheritance of a B10-derived allele: a χ^2 value of 10.3 centered on Ch13 at *D13mit39* (37 cM) and a χ^2 value of 8.1 centered on Ch14 at *D14mit109* (3.3 cM). These four regions correspond to loci previously associated with autoimmunity in NOD mice, as discussed below, and mathematical modeling was consistent with an additive interaction among these loci and those identified on Ch1 and Ch2 (Supplemental Data). Thus NOD resistance to thymic deletion is a complex polygenic trait.

Discussion

The findings here pinpoint the cellular and molecular action of a subset of autoimmune loci in the NOD strain, showing that they cause a general, quantitative resistance to thymic deletion in vivo across a range of thymic developmental subsets and thymic antigen sources and amounts. In vivo mRNA analysis reveals that the NOD genes cause a remarkably selective failure of thymic autoantigen to induce *Bim*, which is an essential, gene dose-limiting mediator of thymic deletion (Bouillet et al., 2002; Villunger et al., 2004). Flow cytometric analysis shows that Bim protein is indeed induced in single T cells

A

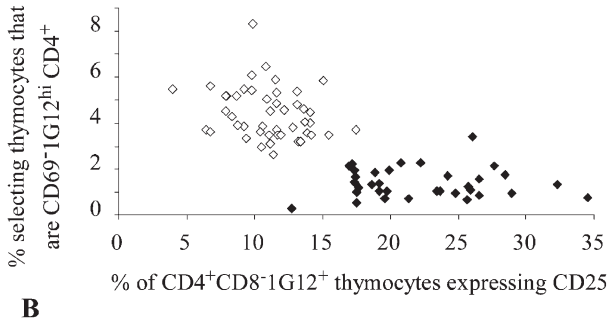

B

Chr	Marker	Location	Deletors Het.	Deletors Ho.	Non-deletors Het.	Non-deletors Ho.	χ^2>4	p
1	D1Mit65	8.4cM	22	13	23	29		
	D1Mit74	31.3cM	20	15	24	28		
Idd5	D1Mit181	42.6cM	23	12	22	30	4.6	0.03
	D1Mit132	43.1cM	21	14	22	30		
	D1Mit191	63.1cM	16	19	23	29		
	D1Mit15	87.9cM	15	20	21	31		
	D1Mit155	112cM	14	21	29	23		
2	D2Mit429	5.0cM	17	18	18	34		
Bim								
Idd13	D2Mit490	64.5cM	23	12	21	31	5.4	0.02
	D2Mit164	71.0cM	24	11	25	27		
	D2Mit504	91.8cM	18	17	25	27		
3	D3Mit267	6.7cM	18	17	29	23		
Idd3	D3nds36	19.2cM	15	20	26	26		
	D3Mit100	45.8cM	13	22	21	31		
Idd10	D3Mit12	49.2cM	13	22	20	32		
Idd18	D3Mit106	55.0cM	13	22	21	31		
	D3Mit127	70.3cM	11	24	25	27		
4	D4Mit172	8.6cM	24	11	31	21		
Idd11	D4Mit76	55.7cM	18	17	25	27		
Idd9	D4Mit233	75.5cM	14	21	22	30		
	D4Mit180	81.0cM	14	21	19	33		
5	D5Mit348	8.0cM	transgene integration					
	D5Mit391	26.0cM	23	12	36	16		
	D5Mit338	59.0cM	18	17	31	21		
	D5Mit31	78.0cM	14	21	28	24		
6	D6Mit183	26.5cM	16	19	21	31		
Idd20	D6Mit102	38.5cM	19	16	21	31		
Idd19	D6Mit254	60.6cM	18	17	21	31		
Idd6	D6Mit374	74.0cM	18	17	18	34		
7	D7Mit178	0.5cM	18	17	29	23		
Idd7	D7Mit76	3.4cM	19	16	30	22		
	Colour	44cM	24	11	19	33	8.6	0.003
	D7Mit101	60.0cM	25	10	18	34	11.3	0.0008
	D7Mit105	63.5cM	24	11	18	34	9.7	0.002
8	D8Mit224	17.0cM	24	11	25	27		
	D8Mit144	31.0cM	23	12	28	24		
Idd22	D8Mit56	73.0cM	19	16	28	24		
9	D9Mit323	6.0cM	21	14	28	24		
Idd2	D9Mit328	23.0cM	22	13	29	23		
	D9Mit50	49.0cM	22	13	28	24		
	D9Mit120	69.0cM	18	17	25	27		
10	D10Mit167	4.0cM	23	12	29	23		
	D10Mit198	40.4cM	24	11	30	22		
	D10Mit42	44.0cM	18	17	20	32		
	D10Mit264	20.0cM	18	17	22	30		
11	D11Mit78	2.0cM	19	16	29	23		
	D11Mit349	32.0cM	15	20	29	23		
	D11Mit298	40.0cM	14	21	22	30		
Idd4	D11Mit38	49.0cM	14	21	22	30		
12	D12Mit136	13.0cM	32	3	44	8		
	D12Mit36	28.0cM						
	D12Mit192	32.0cM	transgene integration					
	D12Mit101	50.0cM	26	9	45	7		
13	D13Mit163	11.0cM	17	18	25	27		
Idd14	D13Mit39	37.0cM	8	27	30	22	10.3	0.001
	D2Mit144	~41cM	10	25	32	20	9.1	0.003
	D13Mit74	59.0cM	16	19	35	17	4.0	0.04
	D13Mit78	75.0cM	12	23	32	20	6.2	0.01
14								
Idd8	D14Mit109	3.0cM	10	25	31	21	8.1	0.004
	D14Mit50	4.0cM	10	25	29	23	6.3	0.01
Idd12	D14Mit37	27.5cM	11	24	32	20	7.6	0.006
	D14Mit95	54.0cM	16	19	32	20		
15	D15Mit176	10.6cM	25	10	25	27	4.7	0.03
	D15Mit229	22.0cM	26	9	21	31	9.7	0.002
	D15Mit29	42.8cM	24	11	19	33	8.6	0.003
	D15Mit161	69.2cM	21	14	20	32		
16	D16Mit131	4.3cM	18	17	28	24		
	D16Mit211	23.3cM	17	18	29	23		
	D16Mit203	55.0cM	15	20	30	22		
17	D17Mit187	47.4cM	congenic interval					
18	D18Mit135	16.0cM	17	18	25	27		
Idd21	D18Mit202	22.0cM	17	18	26	26		
	D18Mit51	37.0cM	17	18	27	25		
	D18Mit4	57.0cM	19	16	30	22		
19	D19Mit59	0.5cM	20	15	27	25		
	D19Mit60	15.0cM	19	16	29	23		
	D19Mit19	26.0cM	15	20	29	23		
	D19Mit33	53.0cM	13	22	27	25		
X	DXMit16	29.5cM	21	14	20	32		

Figure 7. Linkage Analysis of NOD Resistance to Thymic Deletion

Thymi from 149 female TCR:insHEL B10.Br>NODk backcross 1 mice were analyzed at 6–10 weeks of age for the proportion of mature CD69$^-$ 1G12^{hi} CD4$^+$ single positive cells among CD4+ and CD4+8+ thymocytes and for the proportion of CD4$^+$CD8$^-$ 1G12$^+$ thymocytes expressing

undergoing in vivo thymic deletion to an *Aire*-dependent antigen and that it fails to be induced in corresponding NOD thymocytes. Genetic analysis shows that the *Bim* gene is a candidate for contributing to NOD resistance to thymic deletion, but this quantitative trait nevertheless remains polygenic, illustrating the complexity of autoimmune susceptibility even when reduced to a simpler cellular trait.

The relationship between clonal deletion in the DP subset and in the most mature CD69$^-$ SP subset of thymocytes, across the range of antigen amounts and sources (Figure 2G), suggests a continuous curvilinear function that is quantitatively, but not qualitatively, altered by NOD genes. We propose the following explanation for these data. In the *insHEL* animals, only rare antigen-presenting cells in the medulla and corticomedullary junction display sufficient autoantigen/MHC complexes to induce Bim and trigger apoptosis, and these are encountered infrequently as DP cells wander in the thymic cortex, receive positive selection signals, and migrate into the medulla. Consistent with this hypothesis, less than 50% of single positive cells bearing HEL-reactive TCRs have induced Bim protein in B10.Br insHEL×TCR double transgenic thymi (Figure 6C). Because positive selection and maturation in the medulla appear to take many days (Scollay and Godfrey, 1995), a high proportion of autoreactive thymocytes nevertheless experience a Bim-inducing encounter by the time they reach the most mature CD69$^-$ stage, where much greater culling is evident in insHEL animals. In *TgHEL* animals with greater antigen expression in thymic epithelial cells (Figure 1), more cells at the corticomedullary junction may display enough peptide/MHC to induce Bim, resulting in more frequent apoptosis-inducing encounters within the DP subset. By selectively depressing Bim induction to a given amount of autoantigen (Figure 6C), the NOD genes would be expected to reduce the frequency of cell contacts with sufficient antigen to induce apoptosis, accounting for the shift in deletion in NOD TgHEL animals to mirror deletion in B10 insHEL animals (Figure 2G).

NOD gene interference with Bim induction by autoantigen does not appear to reflect a global interference with TCR signaling in thymocytes, because a range of calcineurin-responsive or ERK-responsive genes in thymocytes are induced normally during positive and negative selection (Figure 5). On the other hand, several other genes that are induced to higher levels during negative selection compared to positive selection (*Nur77*, *NFκB1*, *c-rel*, and *A1*) show significantly blunted induction in NOD cells, although not to the extent of *Bim*, suggesting that qualitative or quantitative changes in TCR signaling may selectively interfere with activation of particular signaling pathways. Because several of these genes are induced by the NFκB pathway (*NFκB1*, *c-rel*, and *A1*) and it has been previously shown that CD28 selectively augments TCR activation of NFκB and negative selection of thymocytes (Punt et al., 1994) and that B7 ligands for CD28 are primarily expressed on medullary, but not cortical, thymic epithelial cells (Degermann et al., 1994), there is the distinct possibility that the NOD alleles dampen the NFκB pathway. A qualitative change in TCR signaling in NOD thymocytes diminishes activation of the zap70-ras-ERK pathway and enhances activation of fyn and phosphorylation of c-cbl (Salojin et al., 1997). It is unclear which TCR signaling pathway is responsible for Bim induction at the transcriptional and protein levels, although intracellular calcium (Bouillet et al., 1999, 2002) and cyclic AMP (Zhang and Insel, 2004) are implicated.

Under these conditions of limiting amount of antigen under the insHEL transgene, it is interesting that we did not observe overexpression of cFLIP in NOD thymocytes, contrary to previous in vitro data (Kishimoto and Sprent, 2001). However, this is not inconsistent with the findings by Kishimoto and Sprent, because the Fas pathway appears to be of greater importance during negative selection toward strong stimuli rather than the weaker stimuli used in the present study (Kishimoto and Sprent, 1999). Taken together, NOD thymocytes may have defects in both the Bim and Fas apoptotic pathways, or a component common to both, with the different pathways coming into play under different circumstances.

Bim is also partially required for thymocyte apoptosis induced by γ irradiation or dexamethasone (Bouillet et al., 2002), and NOD gene interference with Bim induction by these stimuli might explain the resistance of NOD thymocytes to γ irradiation (Bergman et al., 2001) and dexamethasone (Bergman et al., 2003). Resistance to dexamethasone maps to the *Idd6* region on distal Ch6, which showed insignificant association with resistance to deletion (Figure 7), whereas NOD resistance to γ radiation-induced apoptosis maps to the *Idd5* region of Ch1. The *Ctla4* gene within this interval is a candidate for radiation resistance because *Ctla4*-deficient thymocytes are also radiation resistant (Bergman et al., 2001). The NOD *Idd5* haplotype produces less of an alternatively spliced *Ctla4* gene product that is a constitutively active inhibitor of TCR zeta phosphorylation (Ueda et al., 2003; Vijayakrishnan et al., 2004). The orthologous region in humans also contains a CTLA-4 variant and has been associated with diabetes, thyroid autoimmunity, Addison's disease, and disease severity in multiple sclerosis (Ueda et al., 2003). The association between the *Idd5* region and in vivo resistance to thymic deletion is significant at $p = 0.03$ tested as a single hypothesis, and the likelihood that this is a true positive is strengthened by the independent evidence associating this locus with autoimmune susceptibility. Further confirmation and analysis of this and the other associated NOD loci will nevertheless require the slow process of breeding NOD congenic TCR×insHEL animals.

The association between resistance to thymic dele-

CD25 as in Figures 2 and 3. Individuals were classified as nondeletors (25%, n = 52), intermediates (42%), or deletors (24%, n = 35) by comparison to NODk and F1 controls. (A) Scatterplot showing separation of deletor and nondeletor mice. (B) Genotype data with *Idd* loci (primary loci tested shown in bold) and marker positions on each chromosome from MGI v3. χ^2 scores are shown when >4. Probabilities shown are for single point values not corrected for multiple testing. Hom, homozygous for NOD allele; Het, heterozygous for NOD and B10 allele.

tion and the region around *D2mit490* at 64.5 cM on Ch2 is also supported by independent evidence. The *Bim* gene lies 11 Mb/5.5 cM proximal to *D2mit490*, making it a good candidate gene for this association. *Bim* is at 128.4 Mb (ENSEMBL), within the boundaries of the B6-derived *Idd13* locus determining diabetes resistance in the NOD-derived strain, NOR (Serreze and Leiter, 1994), and is within the proximal Idd13 sublocus as determined by subcongenic strains (Serreze et al., 1998) along with a diabetes-modifying polymorphism in β-2 microglobulin (Hamilton-Williams et al., 2001; Serreze et al., 1998). The association of resistance to thymic deletion with NOD alleles at Ch2 *Idd13* and Ch1 *Idd5* is notable, because these two loci act cooperatively in promoting T cell influx into pancreatic islets (Fox et al., 2000).

Resistance to thymic deletion was strongly associated with NOD-derived loci on Ch7 at *D7mit101* (60 cM) and on Ch15 at *D15mit229* (22.2 cM). The Ch7 region corresponds to a NOD-derived diabetes susceptibility loci defined by McDuffie in a subcongenic strain (McDuffie, 2000) and to a locus at 58.7 cM, *Ssial3*, contributing to development of autoimmune sialoadenitis in a NOD×NZW cross (Boulard et al., 2002). The fact that this region has not been linked to diabetes in NOD×B10 crosses could be explained by the presence of a B10 diabetes susceptibility locus, *Idd7*, at the proximal end of Ch7 (Ghosh et al., 1993), which would interfere with detection of linked NOD susceptibility loci and is absent from the subcongenic diabetes-resistant strain (McDuffie, 2000). The Ch15 locus corresponds to a region showing suggestive evidence ($\chi^2 = 5$) for association with diabetes in NOD×B10 (Ghosh et al., 1993). A locus in the same region of Ch15 from the MRL strain, *Paam1* at 18.7 cM, promotes progression of autoimmune arthritis in an MRL.*lpr*×C3H.*lpr* cross (Kamogawa et al., 2002). Nur77 is an unlikely candidate for the Ch15 linkage, because it lies 4 Mb distal of D15Mit161 ($\chi^2 < 4$).

In addition to the four NOD-derived loci associated with resistance to thymic deletion, the trait becomes more complex in the backcross, because two B10-derived loci on Ch13 and Ch14 were also strongly associated with resistance to deletion. Both the location and "polarity" of these loci correspond with two regions where the B10-derived allele paradoxically associates with susceptibility to diabetes in B10×NOD backcross mapping: *Idd8* on Ch14 and an unnamed suggestive locus ($\chi^2 = 5.6$) on Ch13 (Ghosh et al., 1993). These B10-derived loci may account for the observation that B10.Br TCR×insHEL animals develop a low incidence, early-onset, autoantibody-negative diabetes that is clinically distinct from the high-incidence, slower onset, autoantibody-positive diabetes in NODk TCR×insHEL animals and that is genetically distinct, because it is fully suppressed in F1 hybrids (Lesage et al., 2002).

Considering as much as 20%–30% of the autosomal genome lies within 20 cM of an *Idd* locus, it would not be surprising if two of the six loci detected overlap with known *Idd* loci by chance and one in six to overlap with the correct polarity (i.e., NOD versus B10 allele associated with susceptibility). However, the fact that all six loci overlap with correct polarity very compellingly argues that the thymic deletion defect is important to the pathogenesis of diabetes in the NOD mouse.

The chromosomal regions associated with resistance to thymic deletion also match NOD loci associated with altered thymic selection and/or regulation: delayed onset of diabetes in NOD BCD2.5 TCR transgenic mice (Gonzalez et al., 1997) and reduced thymic positive selection of NKT cells in the NOD mouse (Esteban et al., 2003). Both these traits were associated with the *Idd13*/*Bim* region on Ch2. Diabetes in BDC2.5 was also associated with the *Idd5* region on Ch1 and with a region of Ch15 from 24 cM to 50 cM. Reduced thymic selection of NKT cells was associated with the same region of Ch7 (*D7mit101*, 60 cM) identified here. In the NKT study, the NOD alleles at each locus associate with reduced thymic positive selection of NKT cells just as they are associated here with reduced thymic negative selection of conventional CD4+ T cells. In the BDC2.5 study, the NOD alleles at each locus are paradoxically associated with resistance to diabetes. Unlike the 3A9 T cells studied here, BDC2.5 T cells are not deleted by the as-yet unknown islet-derived peptide in either background, and resistance to diabetes depends upon peripheral regulation by other T cell specificities (Gonzalez et al., 2001). BDC2.5 TCR-bearing CD4 cells are less efficiently positively selected on the NOD background (Gonzalez et al., 1997). The concordance of loci mapped in the three studies further strengthens the conclusion that these autoimmunity loci act by interfering with specific TCR signals for thymocyte selection.

The magnitude of the thymic deletion defect caused by the NOD genes is only slightly less severe than that caused by homozygous *Aire* deficiency in the same 3A9 TCR×insHEL strain (Liston et al., 2003), and like *Aire* deficiency in humans and mice, the generality of this defect is likely to play a key part in the susceptibility of NOD-derived strains to a range of different organ-specific diseases. Different autoantigens and tissues may become prime targets for this general defect through variations in other genes such as MHC or B7.2 (Salomon et al., 2001; Todd and Wicker, 2001), perhaps because these other genetic alterations selectively reduce thymic presentation and TCR induction of Bim by particular peptides and further increase the frequency of autoreactive T cells against these targets. Our findings show that it will be important to define the TCR pathway for Bim induction and how it is genetically suppressed in order to develop tests for comparable cellular defects in human autoimmune diseases that might be performed on peripheral blood T cells and to develop drugs that augment this pathway to diminish the incidence of autoimmune disease in individuals with this susceptibility trait.

Experimental Procedures

Mice

3A9 TCR transgenic mice (Ho et al., 1994), ILK-3 ins:mHEL transgenic mice (Akkaraju et al., 1997b), KLK4 H2-K:mHEL transgenic mice (Hartley et al., 1991), TLK3 Tg:mHEL transgenic mice (Akkaraju et al., 1997a, 1997b), and ML4 Mt:sHEL transgenic mice (Adelstein et al., 1991) were produced in C57BL/6J and backcrossed to B10.Br/SgSnJ (JAX) or NOD.H2^k (Podolin et al., 1993). Data presented are from N8–N10 for B10.Br mice and N6 for NODk mice. TCR, HEL, and H2 genotype of each mouse was tested twice by PCR (Akkaraju et al., 1997b). Bim$^{0/0}$ mice were as described (Villunger et al., 2004).

Immunofluorescence and Confocal Microscopy

Frozen thymus sections (8 μm) were fixed on slides in −20°C acetone for 30 s, air dried, washed in PBS, and stained with biotinylated anti-HEL mAb (Hy-9) and rabbit anti-keratin antibodies followed by Alexa-488-conjugated streptavidin and Alexa-568-conjugated anti-rabbit IgG. Images were acquired on a Bio-Rad MRC 1024 confocal microscope with a three-line Kr/Ar laser (excitation lines 488, 568, and 647 nm) by using the Bio-Rad acquisition software LaserSharp version 3.2.

Flow Cytometry

Six- to twelve-week-old nondiabetic mice were analyzed. The following antibodies were used: mouse IgG1 anti-clonotypic 1G12 antibody (Van Parijs et al., 1998) culture supernatant followed by rat monoclonal anti-mouse IgG1 APC, anti-CD8-PerCP, anti-CD4-FITC, anti-CD4-PE, anti-CD25-PE, anti-CD69-PE, anti-Vα2-PE, anti-CD3-PE, and anti-CD5.2-FITC (all from Pharmingen). Staining with 10B12 involved labeling with 1G12, fixing in 1% paraformaldehyde (BDH), and permeabilizing cells for 30 min at 4°C in PBS/0.3% saponin (Sigma)/2% FCS containing anti-Bim mAb clone 10B12 (L.A.O. and A.S., unpublished data) or isotype-matched control mAb (IgG2a, Pharmingen). Cells were washed with 0.03% saponin/2% FCS and incubated with biotinylated anti-rat Ig2a (Pharmingen) in 0.3% saponin. After the cells were washed, Bim was revealed with avidin phycoerthyrin. Data was collected on a FACSCalibur (BD Biosciences) and analyzed with FlowJo software (Treestar).

Microarray Analysis of Sorted Cells

Thymus cell suspensions from 6- to 8-week-old female mice were prepared in RPMI without phenol red and supplemented with 10% foetal calf serum, 10 mM HEPES, 50 units/ml penicillin/streptomycin, 2 mM L-glutamine, 0.1% azide, and 1 mM EDTA containing 5 μg/ml Actinomycin D and 2 μg/ml α-Amanitin (Sigma-Aldrich) to inhibit RNA polymerase action. Cells were stained with CD4-FITC, CD69-PE, CD8-PerCP, 1G12 supernatant, and anti-IgG1-APC and were kept at 4°C throughout the staining procedure. Stained cells were sorted on a Becton Dickinson FACVantage (DiVa) into chilled sorting medium as above, centrifuged, and resuspended in Trizol reagent (Invitrogen). RNA was purified from 10^5–10^6 cells with the Qiagen RNeasy kit, and two rounds of in vitro RNA amplification were performed. Sample preparation followed the Affymetrix GeneChip Eukaryotic Small Sample Target Labeling Assay Version II protocol. The first cycle IVT was performed with MEGAscript (Ambion), and the second round IVT was performed with the ENZO BioArray HighYield RNA Transcript Labeling kit (Affymetrix) according to the protocol. Labeled cRNA was fragmented and hybridised to Affymetrix GeneChip 430A arrays (Santa Clara, CA). GeneChips were washed, stained, scanned as per manufacturer's recommendation, and analyzed with MAS5 (Affymetrix).

Genetic Mapping

Thymi from 6–10-week-old nondiabetic TCR:insHEL female backcross mice were analyzed by flow cytometry in batches of five to fifteen normalizing the mean of the batch to the mean of the entire data set to remove batch-related variation. Microsatellite markers were chosen based on identified linkage to diabetes susceptibility in the NOD mouse. Additional markers from the MIT database were chosen based on genomic spacing and reliable discrimination between the B10.Br and NODk strains. *D2mit144* was repositioned on Ch13 (Esteban et al., 2003). Primers were from GeneWorks (Adelaide, Australia), and PCR reactions were resolved by agarose gel electrophoresis. Analysis of linkage was performed in Prism (GraphPad) with χ^2 2 × 2 contingency tables testing the ratio of homozygous to heterozygous mice in the two extreme phenotypes deletor and nondeletor.

Acknowledgments

We thank M. Jordan for advice; G. Hoyne and O. Siggs for critically reading this manuscript; L. Wicker, E. Unanue, and D. Peterson for generous gifts of mice and antibody; D. Buckle and D. Howard for microsatellite analysis; G. Osborne and S. Gruninger for FACS expertise; H. Wilson for assistance with Affymetrix hybridisation; K. Sullivan, R. Gambell, and the staff of Australian Phenomics Facility for curating the mouse colony; and K. Pulsford, D. Howard, and S. Ewing for genotyping. We also thank D. Huang (Walter and Eliza Hall Institute) for assistance in raising the anti-Bim mAb. This work was supported by grants from the National Health and Medical Research Council (NHMRC) and the Juvenile Diabetes Research Foundation. L.A.O. is a recipient of the R.D. Wright Biomedical Career Development Award (NHMRC).

Received: July 29, 2004
Revised: October 17, 2004
Accepted: October 20, 2004
Published: December 14, 2004

References

Adelstein, S., Pritchard-Briscoe, H., Anderson, T.A., Crosbie, J., Gammon, G., Loblay, R.H., Basten, A., and Goodnow, C.C. (1991). Induction of self-tolerance in T cells but not B cells of transgenic mice expressing little self antigen. Science *251*, 1223–1225.

Akkaraju, S., Canaan, K., and Goodnow, C.C. (1997a). Self-reactive B cells are not eliminated or inactivated by autoantigen expressed on thyroid epithelial cells. J. Exp. Med. *186*, 2005–2012.

Akkaraju, S., Ho, W.Y., Leong, D., Canaan, K., Davis, M.M., and Goodnow, C.C. (1997b). A range of CD4 T cell tolerance: partial inactivation to organ-specific antigen allows nondestructive thyroiditis or insulitis. Immunity *7*, 255–271.

Anderson, M.S., Venanzi, E.S., Klein, L., Chen, Z., Berzins, S., Turley, S.J., Von Boehmer, H., Bronson, R., Dierich, A., Benoist, C., and Mathis, D. (2002). Projection of an immunological self shadow within the thymus by the sire protein. Science *298*, 1395–1401.

Bergman, M.L., Cilio, C.M., Penha-Goncalves, C., Lamhamedi-Cherradi, S.E., Lofgren, A., Colucci, F., Lejon, K., Garchon, H.J., and Holmberg, D. (2001). CTLA-4−/− mice display T cell-apoptosis resistance resembling that ascribed to autoimmune-prone non-obese diabetic (NOD) mice. J. Autoimmun. *16*, 105–113.

Bergman, M.L., Duarte, N., Campino, S., Lundholm, M., Motta, V., Lejon, K., Penha-Goncalves, C., and Holmberg, D. (2003). Diabetes protection and restoration of thymocyte apoptosis in NOD Idd6 congenic strains. Diabetes *52*, 1677–1682.

Bouillet, P., Metcalf, D., Huang, D.C., Tarlinton, D.M., Kay, T.W., Kontgen, F., Adams, J.M., and Strasser, A. (1999). Proapoptotic Bcl-2 relative Bim required for certain apoptotic responses, leukocyte homeostasis, and to preclude autoimmunity. Science *286*, 1735–1738.

Bouillet, P., Purton, J.F., Godfrey, D.I., Zhang, L.C., Coultas, L., Puthalakath, H., Pellegrini, M., Cory, S., Adams, J.M., and Strasser, A. (2002). BH3-only Bcl-2 family member Bim is required for apoptosis of autoreactive thymocytes. Nature *415*, 922–926.

Boulard, O., Fluteau, G., Eloy, L., Damotte, D., Bedossa, P., and Garchon, H.J. (2002). Genetic analysis of autoimmune sialadenitis in nonobese diabetic mice: a major susceptibility region on chromosome 1. J. Immunol. *168*, 4192–4201.

Choisy-Rossi, C.M., Holl, T.M., Pierce, M.A., Chapman, H.D., and Serreze, D.V. (2004). Enhanced pathogenicity of diabetogenic T cells escaping a non-MHC gene-controlled near death experience. J. Immunol. *173*, 3791–3800.

Degermann, S., Surh, C.D., Glimcher, L.H., Sprent, J., and Lo, D. (1994). B7 expression on thymic medullary epithelium correlates with epithelium-mediated deletion of V beta 5+ thymocytes. J. Immunol. *152*, 3254–3263.

Esteban, L.M., Tsoutsman, T., Jordan, M.A., Roach, D., Poulton, L.D., Brooks, A., Naidenko, O.V., Sidobre, S., Godfrey, D.I., and Baxter, A.G. (2003). Genetic control of NKT cell numbers maps to major diabetes and lupus loci. J. Immunol. *171*, 2873–2878.

Fox, C.J., Paterson, A.D., Mortin-Toth, S.M., and Danska, J.S. (2000). Two genetic loci regulate T cell-dependent islet inflammation and drive autoimmune diabetes pathogenesis. Am. J. Hum. Genet. *67*, 67–81.

Ghosh, S., Palmer, S.M., Rodrigues, N.R., Cordell, H.J., Hearne,

C.M., Cornall, R.J., Prins, J.B., McShane, P., Lathrop, G.M., Peterson, L.B., et al. (1993). Polygenic control of autoimmune diabetes in nonobese diabetic mice. Nat. Genet. *4*, 404–409.

Gonzalez, A., Katz, J.D., Mattei, M.G., Kikutani, H., Benoist, C., and Mathis, D. (1997). Genetic control of diabetes progression. Immunity *7*, 873–883.

Gonzalez, A., Andre-Schmutz, I., Carnaud, C., Mathis, D., and Benoist, C. (2001). Damage control, rather than unresponsiveness, effected by protective DX5+ T cells in autoimmune diabetes. Nat. Immunol. *2*, 1117–1125.

Hamilton-Williams, E.E., Serreze, D.V., Charlton, B., Johnson, E.A., Marron, M.P., Mullbacher, A., and Slattery, R.M. (2001). Transgenic rescue implicates beta2-microglobulin as a diabetes susceptibility gene in nonobese diabetic (NOD) mice. Proc. Natl. Acad. Sci. USA *98*, 11533–11538.

Hartley, S.B., Crosbie, J., Brink, R., Kantor, A.B., Basten, A., and Goodnow, C.C. (1991). Elimination from peripheral lymphoid tissues of self-reactive B lymphocytes recognizing membrane-bound antigens. Nature *353*, 765–769.

Ho, W.Y., Cooke, M.P., Goodnow, C.C., and Davis, M.M. (1994). Resting and anergic B cells are defective in CD28-dependent costimulation of naive CD4+ T cells. J. Exp. Med. *179*, 1539–1549.

Jordan, M.S., Boesteanu, A., Reed, A.J., Petrone, A.L., Holenbeck, A.E., Lerman, M.A., Naji, A., and Caton, A.J. (2001). Thymic selection of CD4+CD25+ regulatory T cells induced by an agonist self-peptide. Nat. Immunol. *2*, 301–306.

Kamogawa, J., Terada, M., Mizuki, S., Nishihara, M., Yamamoto, H., Mori, S., Abe, Y., Morimoto, K., Nakatsuru, S., Nakamura, Y., and Nose, M. (2002). Arthritis in MRL/lpr mice is under the control of multiple gene loci with an allelic combination derived from the original inbred strains. Arthritis Rheum. *46*, 1067–1074.

Kishimoto, H., and Sprent, J. (1999). Strong TCR ligation without costimulation causes rapid onset of Fas-dependent apoptosis of naive murine CD4+ T cells. J. Immunol. *163*, 1817–1826.

Kishimoto, H., and Sprent, J. (2001). A defect in central tolerance in NOD mice. Nat. Immunol. *2*, 1025–1031.

Lesage, S., Hartley, S.B., Akkaraju, S., Wilson, J., Townsend, M., and Goodnow, C.C. (2002). Failure to censor forbidden clone of CD4 T cells in autoimmune diabetes. J. Exp. Med. *196*, 1175–1188.

Liston, A., Lesage, S., Wilson, J., Peltonen, L., and Goodnow, C.C. (2003). Aire regulates negative selection of organ-specific T cells. Nat. Immunol. *4*, 350–354.

Liston, A., Gray, D.H.D., Lesage, S., Fletcher, A.L., Wilson, J., Webster, K.E., Scott, H.S., Boyd, R.L., Peltonen, L., and Goodnow, C.C. (2004). Gene dosage—limiting role of Aire in thymic expression, clonal deletion and organ-specific autoimmunity. J. Exp. Med. *200*, 1015–1026.

McDuffie, M. (2000). Derivation of diabetes-resistant congenic lines from the nonobese diabetic mouse. Clin. Immunol. *96*, 119–130.

McHugh, R.S., Shevach, E.M., and Thornton, A.M. (2001). Control of organ-specific autoimmunity by immunoregulatory CD4(+)CD25(+) T cells. Microbes Infect. *3*, 919–927.

Podolin, P.L., Pressey, A., DeLarato, N.H., Fischer, P.A., Peterson, L.B., and Wicker, L.S. (1993). I-E+ nonobese diabetic mice develop insulitis and diabetes. J. Exp. Med. *178*, 793–803.

Punt, J.A., Osborne, B.A., Takahama, Y., Sharrow, S.O., and Singer, A. (1994). Negative selection of CD4+CD8+ thymocytes by T cell receptor-induced apoptosis requires a costimulatory signal that can be provided by CD28. J. Exp. Med. *179*, 709–713.

Puthalakath, H., Huang, D.C., O'Reilly, L.A., King, S.M., and Strasser, A. (1999). The proapoptotic activity of the Bcl-2 family member Bim is regulated by interaction with the dynein motor complex. Mol. Cell *3*, 287–296.

Salojin, K., Zhang, J., Cameron, M., Gill, B., Arreaza, G., Ochi, A., and Delovitch, T.L. (1997). Impaired plasma membrane targeting of Grb2-murine son of sevenless (mSOS) complex and differential activation of the Fyn-T cell receptor (TCR)-zeta-Cbl pathway mediate T cell hyporesponsiveness in autoimmune nonobese diabetic mice. J. Exp. Med. *186*, 887–897.

Salomon, B., Rhee, L., Bour-Jordan, H., Hsin, H., Montag, A., Soliven, B., Arcella, J., Girvin, A.M., Padilla, J., Miller, S.D., and Bluestone, J.A. (2001). Development of spontaneous autoimmune peripheral polyneuropathy in B7-2-deficient NOD mice. J. Exp. Med. *194*, 677–684.

Scollay, R., and Godfrey, D.I. (1995). Thymic emigration: conveyor belts or lucky dips? Immunol. Today *16*, 268–273.

Serreze, D.V., and Leiter, E.H. (1994). Genetic and pathogenic basis of autoimmune diabetes in NOD mice. Curr. Opin. Immunol. *6*, 900–906.

Serreze, D.V., Bridgett, M., Chapman, H.D., Chen, E., Richard, S.D., and Leiter, E.H. (1998). Subcongenic analysis of the Idd13 locus in NOD/Lt mice: evidence for several susceptibility genes including a possible diabetogenic role for beta 2-microglobulin. J. Immunol. *160*, 1472–1478.

Todd, J.A., and Wicker, L.S. (2001). Genetic protection from the inflammatory disease type 1 diabetes in humans and animal models. Immunity *15*, 387–395.

Ueda, H., Howson, J.M., Esposito, L., Heward, J., Snook, H., Chamberlain, G., Rainbow, D.B., Hunter, K.M., Smith, A.N., Di Genova, G., et al. (2003). Association of the T-cell regulatory gene CTLA4 with susceptibility to autoimmune disease. Nature *423*, 506–511.

Van Parijs, L., Peterson, D.A., and Abbas, A.K. (1998). The Fas/Fas ligand pathway and Bcl-2 regulate T cell responses to model self and foreign antigens. Immunity *8*, 265–274.

Vijayakrishnan, L., Slavik, J.M., Illes, Z., Greenwald, R.J., Rainbow, D., Greve, B., Peterson, L.B., Hafler, D.A., Freeman, G.J., Sharpe, A.H., et al. (2004). An autoimmune disease-associated CTLA-4 splice variant lacking the B7 binding domain signals negatively in T cells. Immunity *20*, 563–575.

Villunger, A., Marsden, V.S., and Strasser, A. (2003). Efficient T cell receptor-mediated apoptosis in nonobese diabetic mouse thymocytes. Nat. Immunol. *4*, 717.

Villunger, A., Marsden, V.S., Zhan, Y., Erlacher, M., Lew, A.M., Bouillet, P., Berzins, S., Godfrey, D.I., Heath, W.R., and Strasser, A. (2004). Negative selection of semimature CD4(+)8(-)HSA+ thymocytes requires the BH3-only protein Bim but is independent of death receptor signaling. Proc. Natl. Acad. Sci. USA *101*, 7052–7057. Published online April 26, 2004. 10.1073/pnas.0305757101

Woronicz, J.D., Calnan, B., Ngo, V., and Winoto, A. (1994). Requirement for the orphan steroid receptor Nur77 in apoptosis of T-cell hybridomas. Nature *367*, 277–281.

Xue, Y., Chomez, P., Castanos-Velez, E., Biberfeld, P., Perlmann, T., and Jondal, M. (1997). Positive and negative thymic selection in T cell receptor-transgenic mice correlate with Nur77 mRNA expression. Eur. J. Immunol. *27*, 2048–2056.

Zhang, L., and Insel, P.A. (2004). The pro-apoptotic protein Bim is a convergence point for cAMP/protein kinase A- and glucocorticoid-promoted apoptosis of lymphoid cells. J. Biol. Chem. *279*, 20858–20865. Published online March 2, 2004. 10.1074/jbc.M310643200